Non-coaxial behaviour of sand in drained rotational shear

Comportement non-coaxial de sable drainé en cisaillement rotationnel

Yang L.-T., Yu H.-S., Wanatowski D., Li X.
Nottingham Centre for Geomechanics, University of Nottingham, Nottingham, United Kingdom

ABSTRACT: This paper presents an experimental investigation into the non-coaxial behaviour of saturated sand in rotational shear. A series of drained rotational shear tests has been performed on dense Leighton Buzzard sand in a hollow cylinder apparatus. The degrees of non-coaxiality defined as the deviation between the major principal stress direction and the major principal strain increment direction were analyzed. The test results demonstrate that the mechanical behaviour of sand under rotational shear is generally non-coaxial, and the variation of the non-coaxiality degree shows a periodic trend during the tests. It was also observed that the effective stress ratio has a significant effect on the non-coaxiality of sand. The larger the stress ratio, the lower degree of non-coaxiality is induced. The results also show that the volumetric strain of sand induced by cyclic rotation of principal stress axes is mainly contractive. Most of the volumetric change occurs during the first few rotation cycles and its accumulative rate tends to decrease as the number of cycles increases.

RÉSUMÉ : Cet article détaille une analyse expérimentale du comportement non-coaxial de sable saturé en cisaillement rotationnel. Une série de tests de cisaillement rotationnel drainé sur un sable Leighton Buzzard dense dans une presse triaxiale à cylindre creux a été réalisée. Les degrés de non-coaxialité calculés comme l'écart entre la direction de la contrainte principale majeure et la direction de l'incrément de la déformation principale ont été analysés. Les résultats des tests montrent que le comportement mécanique du sable sous cisaillement rotationnel est généralement non-coaxial, et que la variation du degré de non-coaxialité présente une certaine périodicité au cours des tests. Un impact non-négligeable du rapport de contrainte effective sur la non-coaxialité du sable a également été observé. Plus le rapport de contrainte est grand, plus le degré de non-coaxialité induit est bas. Les résultats montrent également que la déformation volumique du sable induite par rotation des axes principaux de contrainte est essentiellement contractante. La plupart du changement volumique se produit au cours des quelques premiers cycles de rotation et son taux d'accumulation tend à diminuer lorsque le nombre de cycles augmente.

KEYWORDS: non-coaxiality, HCA, drained rotational shear, sand

1 INTRODUCTION.

Non-coaxial behaviour refers to the non-coincidence of principal stress directions and principal plastic strain rate directions (Yu 2008). Evidenced by many laboratory observations, granular materials, like sand, often exhibit non-coaxial behaviour (Roscoe et al. 1967, Symes et al. 1984, Arthur et al. 1986, Gutierrez et al. 1991). In many practical situations, ignoring the effects of soil non-coaxiality may be unsafe (Yu and Yuan 2006).

Many loading situations such as those induced by earthquakes, traffic loading and sea waves involve cyclic rotation of principal stress axes. Extensive experimental studies on principal stress rotation have been carried out on granular soils over the past few decades (e.g., Ishihara and Towhata 1983, Symes et al. 1984, Nakata et al. 1998, Yang et al. 2007, Tong et al. 2010). Several test results have shown the significant effect of principal stress rotation on the response of soil specimens. Plastic deformations as well as non-coaxiality between the principal directions of stress and strain increment can be induced due to principal stress axes' rotation.

Until now, most studies on soils undergoing cyclic rotation of principal stress axes have mainly focused on the undrained strength, flow deformation and liquefaction behaviour of soils during rotational shear. The cyclic behaviour under drained conditions has not attracted much interest. Very little literature directly addresses the non-coaxial behaviour of sand under cyclic rotation of principal stress axes.

This paper presents an experimental investigation into the non-coaxial behaviour of saturated sand in drained rotational shear. All the tests were performed in a hollow cylinder apparatus (HCA) which allows an independent control of the magnitude of the three principal stresses and the inclination of the major principal stress axis. The degrees of non-coaxiality calculated as the deviation between the major principal stress direction and the principal strain increment direction at different stress ratios during rotational shear were analyzed.

2 TESTING ARRANGMENT AND PROCEDURES

2.1 *Hollow cylinder apparatus*

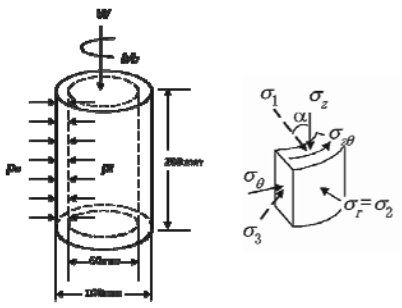

Figure 1. Applied loads and stress components in a hollow cylindrical specimen.

In this study, the HCA, developed by GDS Instruments Ltd, was used. For the details of the testing system, see Cai (2010). The hollow cylindrical specimen had an inner radius of 30 mm, outer radius of 50 mm and height of 200 mm. As shown in Figure 1, the loading of the specimen consisted of an axial load W, torque M_T, inner cell pressure P_i and outer cell pressure P_o. The application of these stress components enables the control of axial stress σ_z, radial stress σ_r, circumferential stress σ_θ, and shear stress $\sigma_{\theta z}$, on an element in the wall of the hollow cylindrical specimen.

Since the stresses are not uniformly distributed across the sample wall especially with unequal inner and outer cell pressures, it is necessary to compute average values. The equations used to calculate the average stress and strain components are listed in Table 1.

Table 1. Equations used to calculate stresses and strains (Hight et al. 1983)

Direction	Stress	Strain
Vertical	$\bar{\sigma}_z = \frac{W}{\pi(r_o^2 - r_i^2)} + \frac{P_o r_o^2 - P_i r_i^2}{r_o^2 - r_i^2}$	$\bar{\varepsilon}_z = \frac{w}{H}$
Circum-ferential	$\bar{\sigma}_\theta = \frac{P_o r_o - P_i r_i}{r_o - r_i}$	$\bar{\varepsilon}_\theta = -\frac{u_0 + u_i}{r_o + r_i}$
Radial	$\bar{\sigma}_r = \frac{P_o r_o + P_i r_i}{r_o + r_i}$	$\bar{\varepsilon}_r = -\frac{u_0 - u_i}{r_o - r_i}$
Shear	$\bar{\sigma}_{\theta z} = \frac{3M_T}{2\pi(r_o^3 - r_i^3)}$	$\bar{\gamma}_{\theta z} = \frac{2\theta(r_o^3 - r_i^3)}{3H(r_o^2 - r_i^2)}$

r_o: outer radius, r_i: inner radius, H: height of specimen, w: axial displacement, u_o: outer radius displacement u_i: inner radius displacement, θ: torsional angle.

The major principal stress, intermediate principal stress and minor principal stress are calculated by using Eqs. (1a)-(1c).

$$\sigma_1 = \frac{\sigma_z + \sigma_\theta}{2} + \sqrt{\left(\frac{\sigma_z - \sigma_\theta}{2}\right)^2 + \sigma_{\theta z}^2} \quad (1a)$$

$$\sigma_2 = \sigma_r \quad (1b)$$

$$\sigma_3 = \frac{\sigma_z + \sigma_\theta}{2} - \sqrt{\left(\frac{\sigma_z - \sigma_\theta}{2}\right)^2 + \sigma_{\theta z}^2} \quad (1c)$$

The stress path in drained tests can be characterized by four independent parameters, namely the mean principal effective stress p', deviatoric stress q, intermediate principal stress parameter b and the angle α_σ between the major principal stress σ_1 and the vertical direction. These parameters are defined in Eqs. (2a)-(2d).

$$p' = \frac{\sigma_1' + \sigma_2' + \sigma_3'}{3} \quad (2a)$$

$$q = \sqrt{\frac{1}{2}\left\{(\sigma_1' - \sigma_2')^2 + (\sigma_1' - \sigma_3')^2 + (\sigma_2' - \sigma_3')^2\right\}} \quad (2b)$$

$$b = \frac{\sigma_2' - \sigma_3'}{\sigma_1' - \sigma_3'} \quad (2c)$$

$$\alpha_\sigma = \frac{1}{2}\tan^{-1}\left(\frac{2\bar{\sigma}_{\theta z}}{\bar{\sigma}_z - \bar{\sigma}_\theta}\right) \quad (2d)$$

2.2 *Sample preparation method*

The tests were performed on dense Leighton Buzzard (Fraction B) sand, with an initial relative density of $D_{rf} \approx 70\%$. Leighton Buzzard sand is made up of sub-rounded particles and mainly composed of quartz. It has a specific gravity of 2.65, mean particle size of 0.62 mm, minimum void ratio of 0.52 and maximum void ratio of 0.79 (Cai 2010). The water sedimentation method was employed to prepare all the samples. After saturation, with a Skempton's B value greater than 0.96, specimens were consolidated isotropically under an effective confining stress of p'=200 kPa.

2.3 *Stress paths of drained rotational shear tests*

The stress paths in q - p' and deviatoric stress planes are shown in Figure 2. In the deviatoric stress plane, the vector from the origin has a length equal to the magnitude of the deviatoric stress q and makes an angle of 2α, which is twice the angle of the major principle stress σ_1 makes with the vertical direction. During the tests, the samples were first subjected to monotonic shearing in the vertical direction up to a specified stress ratio (η=0.8, 0.9, 1.0, 1.1) while keeping the effective mean stress p' constant (A→B). After that the principal stress axes were rotated counter clockwise (B→C→D→E→B) under drained condition, while keeping the deviatoric stress constant and maintaining the effective mean stress p'=200 kPa and the intermediate principal stress parameter b=0. To ensure full discharge of water from the specimen, the major principal stress direction α_σ was rotated at a slow rate of 2°/min.

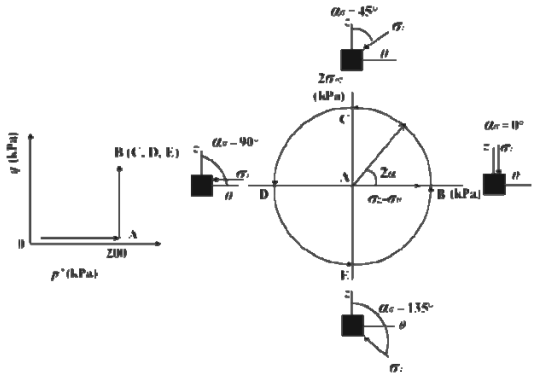

Figure 2. Stress paths for rotational shear test (Nakata et al. 1998).

3 TEST RESULTS AND DISCUSSIONS

3.1 *Development of volumetric strain*

The evolutions of the volumetric strain ε_v with the increasing number of cycles for rotational shear tests are shown in Figure 3. A positive value along the vertical axis indicates contraction and negative indicates dilation. Although the magnitudes of principal stresses were maintained constant during each test, contractive volumetric strain accumulated due to the rotation of principal stress directions. It can be observed that most of the volumetric strain occurs during the first few cycles and its accumulation rate tends to decrease as the number of cycles increases. It is clear that the effect of stress ratio on the development of the volumetric strain is significant under otherwise identical conditions. For all the four tests, the amount of the contractive volumetric strain at the same number of cycles increases with the increase in the stress ratio η.

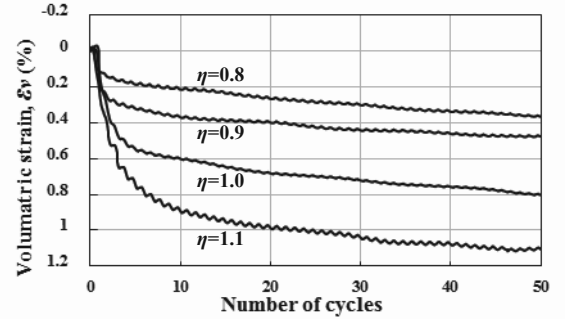

Figure 3. Stress paths for rotational shear test.

3.2 *Non-coaxiality*

The degree of non-coaxiality as measured by the deviation between the major principal stress direction and the principal strain increment direction, ($\alpha_{d\varepsilon}$-α_σ) for tests with different stress ratios are plotted in Figure 4(a) - (d). As elastic strain increment takes a much smaller proportion in the total strain increment compared to that of the plastic strain increment (Gutierrez et al. 1991), the total strain increment instead of the plastic strain increment is used in the following analysis. In general, the variation trend of the non-coaxiality degree shows an obvious oscillation during the tests. Lower degrees of non-coaxiality are observed in the first few cycles. When the rotational shear continues, the strain increment direction becomes closer to the stress increment direction and higher degrees of non-coaxiality are observed. After about 20 rotation cycles, the variation of the non-coaxiality degree appeared to be stabilized. It is clear that the increasing trend of the non-coaxiality degree at the initial stage is more obvious for tests with higher stress ratios.

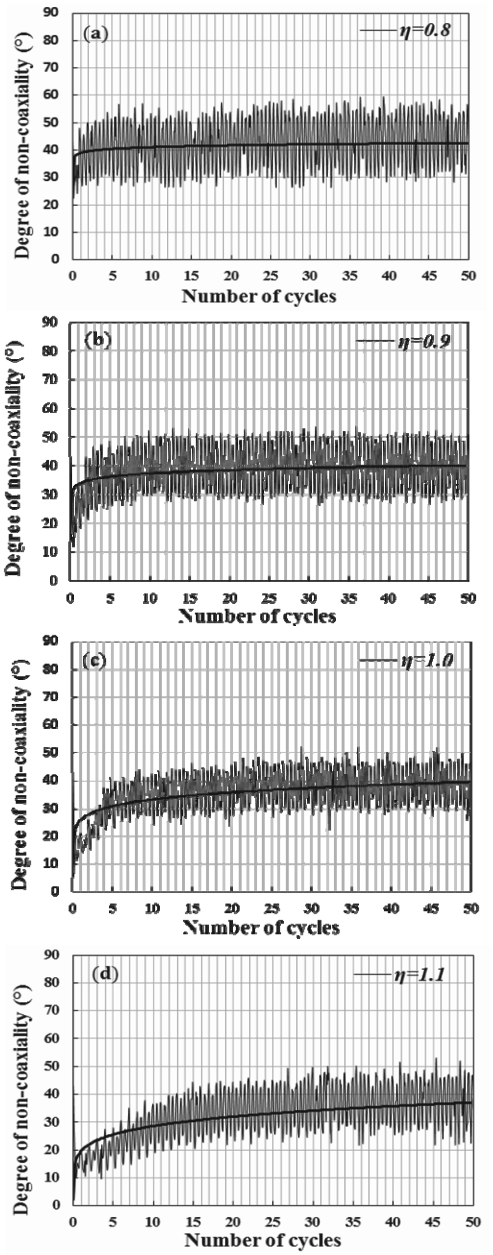

Figure 4. Degree of non-coaxiality against number of cycles for test with: (a) η=0.8; (b) η=0.9; (c) η=1.0; (d) η=1.1.

The black solid lines in Figure 4 are the trend lines of the non-coaxiality degree. With a lower stress ratio (η=0.8), ($\alpha_{d\varepsilon}$-α_σ) is closer to 45°, indicating the strain increment direction is closer to the stress increment direction. At the same number of cycles, the degree of non-coaxiality decreased with the increase of the stress ratio. This observation agrees well with the laboratory results presented by Gutierrez et al. (1991) and numerical results obtained by Li and Yu (2009) based on DEM simulations.

As described above, the variation trend of the non-coaxiality degree shows an obvious periodicity during the tests. To have a better view, the relationship of the non-coaxiality degree with the major principal stress direction α_σ at the cycle numbers N=1 and N=20 are presented in Figure 5(a) and 5(b). Figure 6 shows the corresponding stress paths and strain increments in these tests. It is clear that the variation of the non-coaxiality degree differs significantly at the two stages. At the initial stage when N=1 the degree of non-coaxiality lies approximately in the range of 10 to 40°, as shown in Figure 5(a). It tends to decrease when α_σ rotates from 0 to 90° and then increase during the latter half cycle's rotation. However, at N=20 (Figure 5b), the fluctuation of the non-coaxial degree exhibits two periods of a sine wave displaced at 180 degree intervals. Meanwhile, as mentioned above, the stress ratio has a significant effect on the non-coaxiality degree. The larger the stress ratio, the lower non-coaxial degree between the directions of the strain increment and stress is induced.

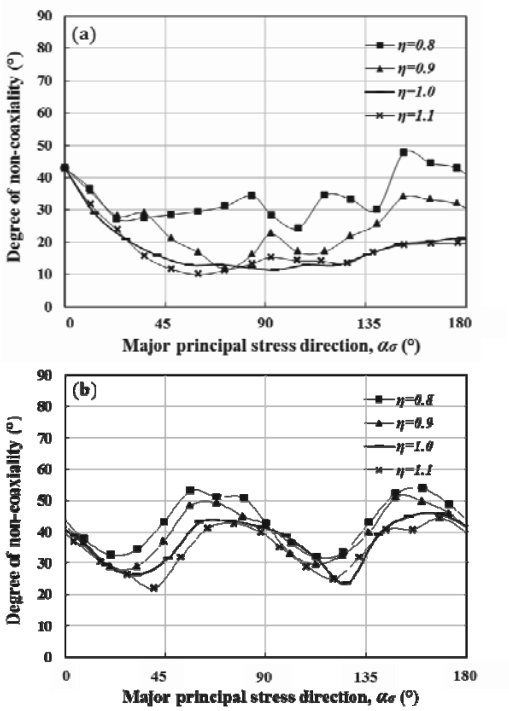

Figure 5. Degree of non-coaxiality for rotational shear tests at: (a) N=1; and (b) N=20.

As shown in Figure 6, for both N=1 and N=20, the directions of the strain increments are gradually enlarged with the increase of the stress ratio. It is interesting to see that for N=20 the strain increment differs significantly in different sections. When the principal stress axes rotate along the stress paths of DA and BC, which correspond to the major principal stress direction α_σ in ranges of [45°, 90°] and [135°, 180°], the strain increment direction almost coincides with the stress increment direction. Similar results have been reported by Tong et al. (2010). For lower stress ratios such as η=0.8 and 0.9 in Figure 6, several arrows pointed inside the cycle, indicating the strain increment

direction is larger than the stress increment direction. However, when the principal stress axes rotate along the stress paths of AB and CD, corresponds to α_σ in ranges of [0°, 45°] and [90°, 135°], the directions of the strain increments are larger and the non-coaxiality between the directions of the strain increment and stress are induced.

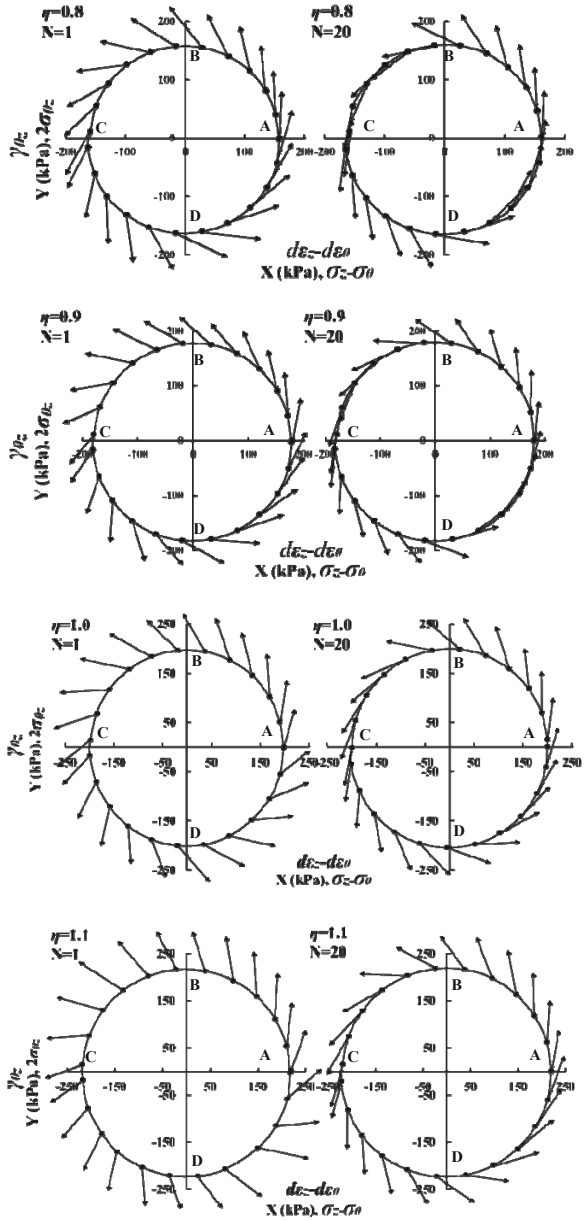

Figure 6. Stress paths and strain increments in rotational shear tests at N=1 and N=20.

4 CONCLUSIONS

This paper presents an experimental investigation of drained behaviour of saturated Leighton Buzzard sand in rotational shear. The samples were subjected to cyclic rotation of principal stress axes while the magnitudes of mean stress and shear stress were maintained constant. A special attention of the investigation has been placed on the non-coaxiality of granular soil subjected to the continuous rotation of major principal stress axis at different stress ratios. The conclusions drawn are as follows:

- The volumetric strain induced by cyclic rotation of principal stress axes is mainly contractive. Most of the contractive volumetric strain occurs during the first few cycles and its accumulation rate tends to decrease as the number of cycles increases. The accumulated volumetric strain increases with the increase in the stress ratio.
- The mechanical behaviour of sand under rotational shear is generally non-coaxial, and the variation trend of the non-coaxiality degree shows an obvious periodicity during the tests.
- Lower degrees of non-coaxiality are observed in the first few cycles. When the rotational shear continues, the strain increment direction becomes closer to the stress increment direction and higher degrees of non-coaxiality are observed. The variation of the non-coaxial degree appeared to be stabilized after approximately 20 cycles of shearing.
- It was also observed that the stress ratio has a significant effect on the non-coaxiality. The larger the stress ratio, the lower degree of non-coaxiality between the directions of the strain increment and stress is induced.

5 REFERENCES

Arthur, J. R. F, Koenders M. A. and Wong R. K. S. 1986. Anisotropy in particle contacts associated with shearing in granular media. Acta Mechanica, 64, 20-29.

Cai Y. 2010. An experimental study of non-coaxial soil behaviour using hollow cylinder testing. Ph.D thesis. University of Nottingham, UK.

Gutierrez M., Ishihara K., and Towhata I. 1991. Flow theory for sand during rotation of principal stress direction. Soils Found., 31 (4), 121-132.

Hight D. W., Gens A., and Symes M. J. 1983. The development of a new hollow cylinder apparatus for investigating the effects of principal stress rotation in soils. Geotechnique, 33 (4), 355–383.

Ishihara K. and Towhata K. 1983. Sand response to cyclic rotation of principal stress directions as induced by wave loads. Soils Found. 23 (4), 11–26.

Roscoe, K. H., Bassett, R. H., and Cole, E. R. L. 1967. Principal axes observed during simple shear of a sand. Proc. 4th Eur. Conf. Soil Mech. Found. Eng., Oslo, 231-237.

Symes, M. J., Gens, A., and Hight, D. W. 1984. Undrained anisotropy and principal stress rotation in saturated sand. Géotechnique, 34 (1), 11-27.

Li X., Yu H.S. 2010. Numerical investigation of granular material behaviour under rotation shear. Geotechnique, 60 (5), 381-394.

Nakata Y., Hyodo M., Murata H. & Yasufuku N. 1998. Flow deformation of sands subjected to principal stress rotation. Soils Found. 38 (2), 115–128.

Tong Z. X., Zhang J-M, Yu Y. L., Zhang G. 2010. Drained deformation behavior of anisotropic sands during cyclic rotation of stress principal axes. J. Geotchanical and Geoenviromental Engineering. ASCE. 136 (11), 1509–1518.

Yang Z. X., Li X. S. and Yang J. 2007. Undrained anisotropy and rotational shear in granular soil. Geotechnique, 57 (4), 371– 384.

Yu, H. S. 2008. Non-coaxial theories of plasticity for granular materials. Proc. 12th Int. Conf. of Int. Assoc. Comp. Meth. Adv. Geom. (IACMAG), Goa, India, 361-378.

Yu, H. S., and Yuan, X. 2006. On a class of non-coaxial plasticity models for granular soils. Proc. Royal Soc. A, 462, 725-748.